



New species of *Eurythenes* from hadal depths of the Mariana Trench, Pacific Ocean (Crustacea: Amphipoda)

JOHANNA N. J. WESTON¹*, PRISCILLA CARRILLO-BARRAGAN¹, THOMAS D. LINLEY¹, WILLIAM D. K. REID¹ & ALAN J. JAMIESON¹

¹*School of Natural and Environmental Sciences, Newcastle University, Newcastle Upon Tyne, UK, NE1 7RU*

*Corresponding author: j.weston2@newcastle.ac.uk

Co-authors: priscilla.carrillo-barragan@newcastle.ac.uk; thomas.linley@newcastle.ac.uk;

william.reid@newcastle.ac.uk; alan.jamieson@newcastle.ac.uk

Abstract

Eurythenes S. I. Smith in Scudder, 1882 are one of the largest scavenging deep-sea amphipods (max. 154 mm) and are found in every ocean across an extensive bathymetric range from the shallow polar waters to hadal depths. Recent systematic studies of the genus have illuminated a cryptic species complex and highlighted the benefits of using a combination of morphological and molecular identification approaches. In this study, we present the ninth species, *Eurythenes plasticus* sp. nov., which was recovered using baited traps between the depths 6010 and 6949 m in the Mariana Trench (Northwest Pacific Ocean) in 2014. This new *Eurythenes* species was found to have distinct morphological characteristics and be a well-supported clade based on sequence variation at two mitochondrial regions (16S rDNA and COI). While this species is new to science and lives in the remote hadal zone, it is not exempt from the impacts of anthropogenic pollution. Indeed, one individual was found to have a microplastic fibre, 83.74% similar to polyethylene terephthalate (PET), in its hindgut. As this species has a bathymetric range spanning from abyssal to hadal depths in the Central Pacific Ocean basin, it offers further insights into the biogeography of *Eurythenes*.

Keywords: Deep sea, integrated taxonomy, cryptic species, molecular phylogeny, microplastic fibre, pollution

Introduction

While the deep sea is one of the largest ecosystems on Earth, it has traditionally been perceived as a homogenous environment, with few barriers to gene flow (Madsen 1961; Charette & Smith 2010). This led to the assumption that many deep-sea species are cosmopolitan, with several appearing to have large geographical and bathymetrical ranges (>3000 m; King & Priede 2008; Brandt *et al.* 2012; Jamieson *et al.* 2013). The deep sea, however, has a high degree of topographic complexity including mid-oceanic ridges, submarine canyons, seamounts, and subduction trenches, which could act as barriers. These barriers potentially restrain gene flow and promote allopatric speciation (Palumbi 1994). This cosmopolitan species concept has now been challenged on several occasions by genetic techniques, whereby widespread deep-sea species are in fact comprised of species complexes with several cryptic or pseudocryptic species (Garlitska *et al.* 2012; Cornils & Held 2014).

The lysianassoid amphipod, *Eurythenes gryllus* (Lichtenstein in Mandt, 1822), is a quintessential and abundant member of the deep-sea benthic community. *Eurythenes gryllus* has long been considered cosmopolitan with an extensive bathymetric range (184 to 8000 m), which spans the bathyal, abyssal, and hadal zones (Hessler *et al.* 1978; Ingram & Hessler 1987; Thurston *et al.* 2002). However, genetic diversity studies have indicated that *E. gryllus* is not a single species but a species complex (France & Kocher 1992; Havermans *et al.* 2013), with nuclear and mitochondrial DNA sequence data indicating the *gryllus*-complex to be composed of at least nine to twelve distinct clades (Havermans *et al.* 2013; Eustace *et al.* 2016; Havermans 2016). Our initial understanding of *E. gryllus* as a single cosmopolitan deep-sea species is reconceptualised when viewed as a species-complex. This provides a much more nuanced picture of their distribution, amphitropical at bathyal depths, and reveals a patchwork of distribution patterns with the complex's radiation. For example, *Eurythenes maldoror* d'Udekem d'Acoz & Havermans, 2015

(i.e., clade Eg3) is from abyssal depths in all oceans but the Arctic, while *Eurythenes* sp. ‘hadal’ is limited to hadal depths within the Peru-Chile Trench (Eustace *et al.* 2016).

Havermans *et al.* (2013) initiated a reverse taxonomic approach to determine the genetic diversity within the *Eurythenes* genus, whereby a potentially new species is first genetically identified and then the morphological characters are determined (Markmann & Tautz 2005). This resulted in *Eurythenes* S. I. Smith in Scudder, 1882 expanding from four to eight described species since the establishment of the monogeneric family (Stoddart & Lowry 2004). Specifically, *Eurythenes aequailatus* Narhara-Nakano, Nakano & Tomikawa, 2017, *Eurythenes andhakarae* d’Udekem d’Acoz & Havermans, 2015, *E. maldoror*, and *Eurythenes sigmiferus* d’Udekem d’Acoz & Havermans, 2015 were described based on combined molecular and morphological methods. In addition to these described species within the *gryllus*-complex, two species from abyssal and hadal depths of the Peru-Chile Trench are awaiting formal description (Eustace *et al.* 2016) and at least six distinct genetic clades lack morphological examination (e.g., clades Eg7-9; Havermans *et al.* 2013; Havermans 2016). The suite of morphological characters that separate species within the *gryllus*-complex remain unclear and are challenging to observe (d’Udekem d’Acoz & Havermans 2015), which highlights the importance of integrating together molecular and morphological identification approaches.

The evolutionary success of *Eurythenes*, with the exception of the pelagic *Eurythenes obesus* (Chevreux, 1905), has largely been attributed to their scavenging plasticity, from detritivory, intercepting large carcasses, and ingesting mud (Barnard 1962; Ingram & Hessler 1983; Blankenship & Levin 2007; Havermans & Smetacket 2018). However, deep-sea amphipods, including *Eurythenes*, may be particularly susceptible to ingesting microplastics given they are voracious and non-selective scavengers (Hargrave 1985; Blankenship & Levin 2007). Indeed, microplastics fibres have already been found in the hindguts of hadal-dwelling amphipods, including the *Eurythenes* sp. ‘hadal’ from the Peru-Chile Trench at 7050 m (Jamieson *et al.* 2019). Furthermore, every individual of the hadal scavenging amphipod, *Hirondellea gigas* (Birstein & Vinogradov, 1955), examined from the deepest point in the Mariana Trench contained at least one man-made fibre in its hindgut (Jamieson *et al.* 2019). Microplastics are transferred to hadal environment via multiple mechanisms, including direct deposit in carrion, marine snow, and trench sediment consolidation (Taylor *et al.* 2016; Peng *et al.* 2018; Jamieson *et al.* 2019). With the increase in plastic debris entering the deep sea (Schluning *et al.* 2013; Chiba *et al.* 2018), including to full ocean depth (Peng *et al.* 2018; Peng *et al.* 2020), the probability of consuming such pollutants increases. It is highly likely that individuals of other scavenger species residing in the Mariana Trench are similarly susceptible to ingesting microplastics fibres.

In this study, we examined the morphological characteristics and sequence variation at the mitochondrial 16S ribosomal DNA (16S) and cytochrome oxidase I (COI) regions of *Eurythenes* specimens collected from hadal depths in the Mariana Trench, Pacific Ocean and considered their taxonomic placement within the *gryllus*-complex. We describe the ninth species within the genus, *Eurythenes plasticus* sp. nov. We also examined the hindgut for the presence of microplastic fibres to continue to track the reach of this ubiquitous pollutant at hadal depths.

Material and Methods

Specimen Collection

Specimens were collected in November 2014 as part of the HADES–M (HADal Ecosystems Studies) expedition cruise FK141109 on the *R/V Falkor* to Sirena Deep, Mariana Trench, Pacific Ocean. The amphipods were recovered using the full-ocean depth *Hadal-lander* (Jamieson 2015; Linley *et al.* 2016). The *Hadal-lander* was equipped with PVC funnel traps baited with whole mackerel bait (Scombridae) and a temperature and pressure sensor (SBE-39, Sea-Bird Electronics, USA). Pressure was converted to depth (m) following Saunders (1981). Collection sites are shown in Fig. 1 and site details are provided in Table 1. Amphipods were preserved with 70% ethanol upon recovery.

TABLE 1. Collection information for specimens collected on the 2014 cruise FK141109 of the *R/V Falkor*. Included is the number of individuals by gender collected at each depth.

Station	Date	Latitude	Longitude	Depth (m)	Female	Male	Juvenile
LH14	26/11/2014	11.5911°N	144.84730°E	6010	–	1	–
LH15	27/11/2014	11.6071°N	144.8331°E	6142	1	–	–
WT02	14/11/2014	12.64065°N	144.73796°E	6865	1	–	7
WT09	24/11/2014	11.8147°N	144.98580°E	6949	–	–	1

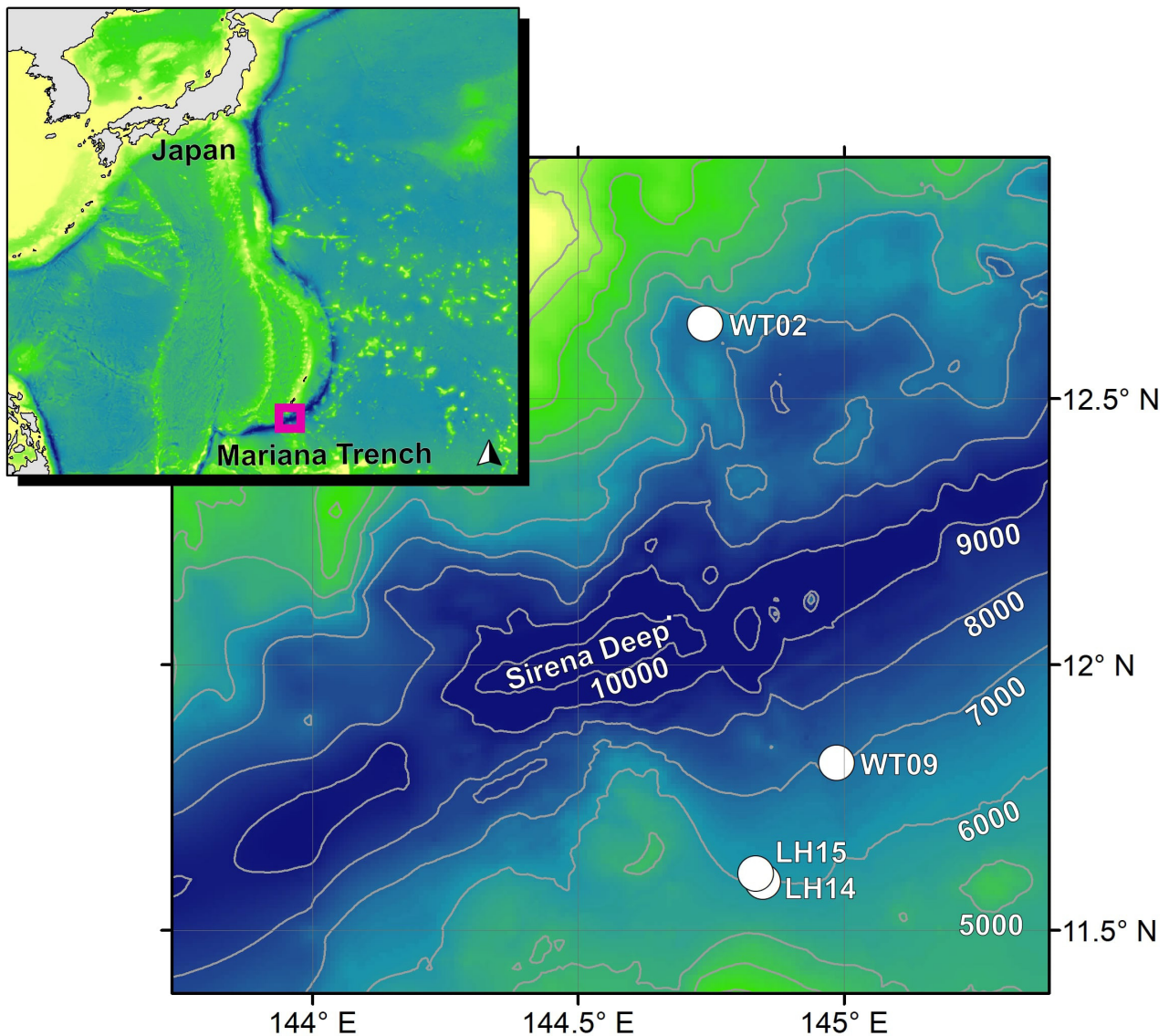


FIGURE 1. Map of sampling stations within across the Sirena Deep, Mariana Trench, Pacific Ocean (white circles). Maps were produced with GEBCO bathymetry data (GEBCO 2015). Isobaths are added for every 1000 m and labelled between 5000 to 10,000 m.

Morphological Assessment and Digital Illustration

Whole specimens were photographed with a Canon EOS 750D DSLR camera, Tamron SP 90 mm f/2.8 VC USD Macro 1:1 VC Lens with polarising filter, and Falcon Eyes CS-730 copy stand and processed with Helicon Focus and Helicon Remote software (Helicon Soft). Body length was measured from the rostrum to the tip of telson. Appendages were dissected using a Wild Heerbrugg M8 stereomicroscope and imaged with a Leica DMi8 inverted microscope and DFC295 camera. Lengths of appendages and articles were measured following Horton & Thurston (2014) to provide consistency regardless of the degree of flexion. Images were converted into digital illustrations using Inkscape v0.92.2 (Coleman 2003; 2009). Type and non-type specimens are deposited at the Smithsonian Institution National Museum of Natural History, Washington, D.C., USA (USNM).

Phylogenetics

Total genomic DNA was extracted from either the head or a pair of pleopods depending on size of the specimen using the Bioline ISOLATE II Genomic DNA Kit. Two partial regions of the mitochondrial DNA were amplified. The 16S (260 bp) was amplified with AMPH1 (France & Kocher 1996) and 'Drosophila-type' 16SBr (Palumbi *et al.* 2002) primers and COI (624 bp) was amplified with LCO1490 and HCO12198 (Folmer *et al.* 1994) primers.

PCR protocols were as described in Ritchie *et al.* (2015). PCR products were purified enzymatically using New England Biolabs Exonuclease 1 and Antarctic Phosphatase and sequenced with an ABI 3730XL sequencer (Eurofins Genomics, Germany).

TABLE 2. Species, sequence accession numbers and references for phylogenetic analysis of *Eurythenes plasticus* sp. nov.

Species	16S	COI	Reference
<i>Alicella gigantea</i>	KP456083	KP713893	Ritchie <i>et al.</i> 2015
<i>Eurythenes aequilatus</i>	LC229090	LC229094	Narahara-Nakano <i>et al.</i> 2017
<i>Eurythenes aequilatus</i>	LC229091	LC229095	Narahara-Nakano <i>et al.</i> 2017
<i>Eurythenes andhakarae</i>	JX887065	JX887114	Havermans <i>et al.</i> 2013
<i>Eurythenes andhakarae</i>	JX887066	JX887119	Havermans <i>et al.</i> 2013
<i>Eurythenes gryllus</i>	JX887060	JX887132	Havermans <i>et al.</i> 2013
<i>Eurythenes gryllus</i>	JX887063	JX887136	Havermans <i>et al.</i> 2013
<i>Eurythenes magellanicus</i>	LC192879	LC192881	Narahara-Nakano <i>et al.</i> 2017
<i>Eurythenes magellanicus</i>	JX887071	JX887144	Havermans <i>et al.</i> 2013
<i>Eurythenes magellanicus</i>	JX887074	JX887145	Havermans <i>et al.</i> 2013
<i>Eurythenes magellanicus</i>	–	KX078274	Havermans 2016
<i>Eurythenes maldoror</i>	JX887069	JX887151	Havermans <i>et al.</i> 2013
<i>Eurythenes maldoror</i>	JX887068	JX887152	Havermans <i>et al.</i> 2013
<i>Eurythenes maldoror</i>	JX887067	JX887121	Havermans <i>et al.</i> 2013
<i>Eurythenes maldoror</i>	KX034310	KX365240	Ritchie <i>et al.</i> 2017
<i>Eurythenes obseus</i>	KP456144	KP713954	Ritchie <i>et al.</i> 2015
<i>Eurythenes plasticus</i> sp. nov.	MT021437	MT038070	This study
<i>Eurythenes plasticus</i> sp. nov.	MT021438	MT038071	This study
<i>Eurythenes plasticus</i> sp. nov.	MT021439	MT038072	This study
<i>Eurythenes sigmiferus</i>	JX887070	–	Havermans <i>et al.</i> 2013
<i>Eurythenes sigmiferus</i>	AY943568	–	Escobar-Briones <i>et al.</i> 2010
<i>Eurythenes thurstoni</i>	U40449	–	France & Kocher 1996
<i>Eurythenes</i> cf. <i>thurstoni</i>	–	KX078272	Havermans 2016
<i>Eurythenes</i> sp. Eg7	U40445	–	France & Kocher 1996
<i>Eurythenes</i> sp. Eg8	U40439	–	France & Kocher 1996
<i>Eurythenes</i> sp. Eg8	U40440	–	France & Kocher 1996
<i>Eurythenes</i> sp. Eg9	U40446	–	France & Kocher 1996
<i>Eurythenes</i> sp. Eg9	U40448	–	France & Kocher 1996
<i>Eurythenes</i> sp. ‘PCT abyssal’	KP456140	KP713957	Ritchie <i>et al.</i> 2015
<i>Eurythenes</i> sp. ‘PCT abyssal’	KP456141	KP713958	Ritchie <i>et al.</i> 2015
<i>Eurythenes</i> sp. ‘PCT hadal’	KP456138	KP713955	Ritchie <i>et al.</i> 2015
<i>Eurythenes</i> sp. ‘PCT hadal’	KP456139	KP713956	Ritchie <i>et al.</i> 2015
<i>Eurythenes</i> sp. 1 (WDL–d1)	–	KX078273	Havermans 2016
<i>Eurythenes</i> sp. 2 (MOZ–1)	–	KX078271	Havermans 2016

Electropherograms were viewed and primers and any ambiguous sequences were trimmed in MEGA 7 (Kumar *et al.* 2016). Sequences were initially blasted using default parameters on NCBI BLASTn. COI sequences were translated into amino acid sequences to confirm that no stop codons were present. Nucleotide alignments with comparative sequences were made using MAFFT v7 (Table 2; Katoh *et al.* 2019). The optimal evolutionary models for each alignment were identified by model test in the *phangorn* 2.4.0 package (Schliep *et al.* 2017). The optimal Akaike Information Criterion and Bayesian Information Criterion indicated the HKY + I + G model for both alignments (Hasegawa *et al.* 1985). Phylogenetic relationships were inferred via the maximum-likelihood approach using PhyML v3.1 (Guidon *et al.* 2010) and the Bayesian approach using BEAST v1.8.4 (Drummond *et al.* 2012). Maximum-likelihood analyses were conducted with a neighbour-joining starting tree and using nearest neighbour interchange branch swapping using the model of sequence evolution and parameters estimated by PhyML. The stability of nodes was assessed from bootstrap support based upon 10,000 iterations. Bayesian analyses were performed for two independent runs of 40,000,000 generations sampling every 10,000 generations using the respective evolutionary models and an uncorrelated relaxed clock (Drummond *et al.* 2006). Outputs were assessed in Tracer v1.7 to ensure convergence (ESS < 200) (Rambaut *et al.* 2018) and combined in Log Combiner v1.8.4. The first

4,000,000 states were discarded. The maximum clade credibility tree was generated through Tree Annotator v1.8.4, viewed in FigTree v1.4.3, and annotated using Inkscape v0.92.2. Two independent methods were used to infer species delimitation on each dataset, specifically a Bayesian Poisson Tree Processes (bPTP) model (Zhang *et al.* 2013) and sequence divergence using the Kimura 2-parameter (K2P) distance model (Kimura 1980).

Sample Digestion and Analysis for Microplastic Ingestion

Preventive measures were taken to reduce and monitor for potential sources of contamination due to the ubiquity of microplastic fibres in the environment (Wesch *et al.* 2017). Samples were prepared and analysed in a clean laboratory with restricted access, where only one researcher, wearing a 100% clean lab coat at all times, was present conducting the experiment. Before any work session, benches were wiped with 70% ethanol on a 100% cotton cloth and allowed to dry fully. Only non-plastic equipment (glass and metal) were used to process the samples. Glass Petri dishes, graduated piston pipettes and test tubes were thoroughly washed with pre-filtered deionised water (DI), rinsed with acetone, covered with aluminium foil and allowed to dry at 70 °C in a drying oven. The digestion and filtration steps were conducted under a laminar flow cabinet (Purair, LS series, Air Science, USA LLC). The equipment and samples were covered wherever possible to minimize environmental exposure. Additionally, procedural blanks were run in parallel with samples to monitor environmental contamination. Meaning, a glass petri dish with a damped Whatman glass fibre filter was left open next to the microscope during the specimens' dissection (Murphy *et al.* 2016), while two empty glass tubes were processed as described below. The resulting three blanks filters were examined under a stereo microscope (Leica M205C, Leica Microsystems GmbH, Germany) to correct for potential air-borne and/or procedural plastic contamination.

Four *E. plasticus* sp. nov. specimens were selected for microplastic analysis: three juveniles (15.1, 15.6, and 23.1 mm body length) from 6865 m and one juvenile (15.6 mm body length) from 6949 m. Each specimen was individually rinsed with pre-filtered DI water and inspected under a stereo microscope (Leica M205C, Leica Microsystems GmbH, Germany), to ensure each specimen was free from external contamination. The hindgut was removed as described in Jamieson *et al.* (2019) and individually placed in 10 mL glass tubes. Aluminium foil was used to cover the tubes. After recording its wet mass, the hindgut was submerged in 10% m/v potassium hydroxide (KOH), using a volume at least three times greater than that occupied by the biological material (Foekema *et al.* 2013). The samples plus two procedural blanks (borosilicate tubes with 2 and 7 mL 10% KOH solution) were incubated for over a 36-hour period at 40 °C. After digestion, samples were left to cool inside a desiccator, following vacuum filtration through 0.6 µm glass fibre filters (Advantec Grade GA55, Advantec MSF Inc., Japan). Filters were individually placed onto a glass Petri dish until further microscopic inspection.

Once dried, glass fibre filters were examined under a stereo microscope. The physical appearance (e.g., colour, shape, size) of the putative particles (e.g., fibre, fragment) per filter was recorded. Said particles were then transferred onto gold plated slides (Thermo Fisher Scientific Inc., UK) for Fourier-transform infrared spectroscopy (FTIR) analysis. A Nicolet iN10 FTIR micro spectroscope (Thermo Fisher Scientific Inc., UK) was employed to obtain the particle's infrared transmittance spectra, using the liquid nitrogen cooled Mercury Cadmium Telluride detector. Results were then visualised and matched against a series of inbuilt reference spectra libraries using the instrument's software (OMNIC Picta v1.7) to determine the chemical identity of the analysed particles.

Results

Phylogenetics and Species Delimitation Analysis

Three specimens of *Eurythenes plasticus* sp. nov. were successfully characterised across the two partial gene amplicons. The sequences have been annotated and deposited into GenBank (Table 2; 16S MT021437–39 and COI MT038070–72).

The phylogenetic relationship of *E. plasticus* sp. nov. within *Eurythenes* was investigated in separate 16S and COI datasets. These comparative datasets were constructed from sequences that are associated with either: type material, specimens identified high degree of confidence, or specimens from a known clade or undescribed lineage (Table 2; France & Kocher 1996; Escobar-Briones *et al.* 2010; Havermans *et al.* 2013; Ritchie *et al.* 2015; Eustace *et al.* 2016; Havermans 2016; Narahara-Nakano *et al.* 2017; Ritchie *et al.* 2017). For the 16S dataset, 26 individuals consisting of the eight species of *Eurythenes* and five genetic clades fit these criteria. For the COI dataset, 25

individuals consisting of seven species of *Eurythenes* and four genetic clades fit these criteria. *Alicella gigantea* Chevreux, 1899 was selected as the outgroup for both datasets. The 16S and COI datasets contained 191 and 394 positions of which 33 and 115 bases were parsimony-informative, respectively.

The Bayesian-based topology based on variation across 16S and COI is shown in Fig. 2. In general, the two topologies shared similar patterns and the differences were largely due to lacking both sets of sequences for a specimen. The COI topology showed *E. plasticus* sp. nov. to form a reciprocally monophyletic group. The 16S topology varied slightly with the inclusion of *Eurythenes* sp. (U40445; France & Kocher 1996) to the *E. plasticus* sp. nov. phylogroup. This *Eurythenes* sp. represents a singleton and recently distinguished as part of the species-level clade Eg7 (Havermans *et al.* 2013). In both topologies, *Eurythenes plasticus* sp. nov. was placed within a larger clade with *E. magellanicus*, *E. aequilatus*, and *Eurythenes* sp. ‘PCT abyssal’. *Eurythenes plasticus* sp. nov. was consistently sister to *E. magellanicus*, with high support in the COI topology (0.99 posterior probability; Fig. 2B).

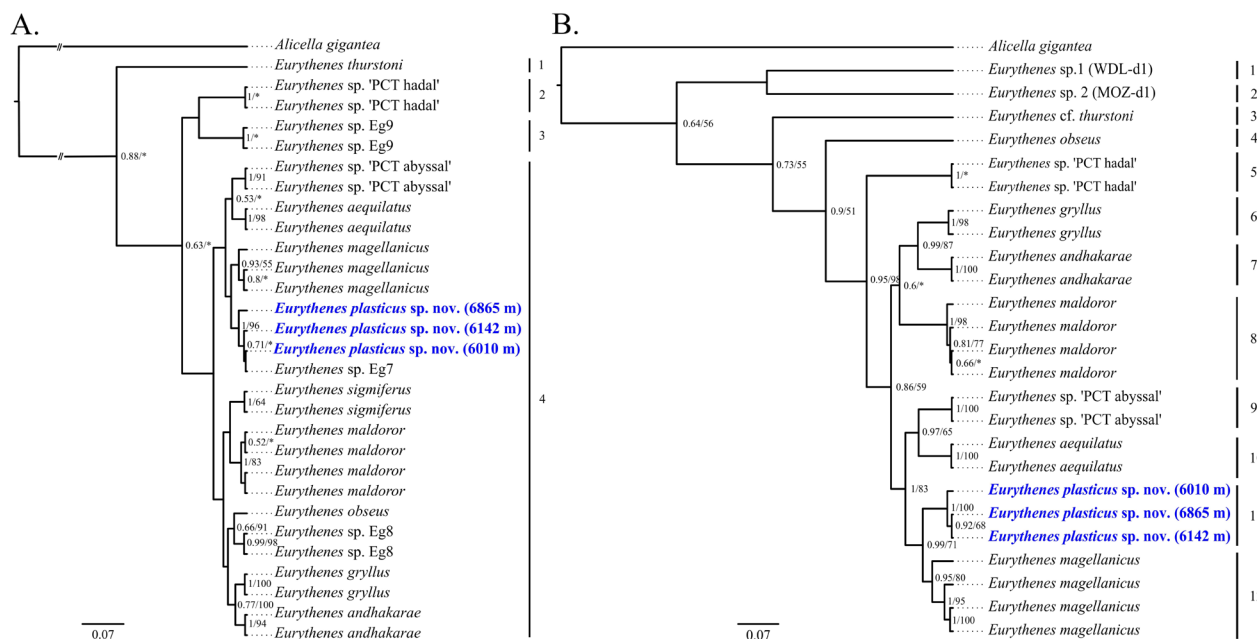


FIGURE 2. Bayesian trees showing the relationship of *E. plasticus* sp. nov. (bold blue) within the *Eurythenes* genus based on: A. 16S rDNA sequence data, and B. COI sequence data. References for comparative sequences are in Table 2. Bayesian posterior probabilities and maximum likelihood bootstrap support are on branch nodes. Values less than 0.50 or 50 are not stated or depicted by asterisk. Species groups determined by bPTP analysis are shown on right side of each phylogeny.

Species delimitation analysis with bPTP for the COI datasets estimated the three specimens of *E. plasticus* sp. nov. to be the same species and distinct from all other *Eurythenes* taxon (mean: 14.33; acceptance rate: 0.0846; estimated number of species: 12–17). The bPTP analysis of the 16S dataset did not delineated *E. plasticus* sp. nov. from *E. magellanicus*, *E. andhakarae*, *E. sigmiferus*, *E. aequilatus*, *E. obseus*, *Eurythenes* sp. ‘PCT abyssal’, and *Eurythenes* spp. Eg7–9 (mean: 5.29; acceptance rate: 0.20456; estimated number of species: 3–13).

With alternative delimitation method, the average K2P estimates of divergence between *E. plasticus* sp. nov. and *E. magellanicus* were 0.034 ± 0.007 for 16S and 0.074 ± 0.008 for COI. The levels of interclade divergence between *E. plasticus* sp. nov. and *E. magellanicus* were comparable to the levels of divergence that have been previously used to detect cryptic speciation within the *gryllus*-complex (Havermans *et al.* 2013; Eustace *et al.* 2016; Narahara-Nakano *et al.* 2017). Furthermore, the ‘4x’ criterion was satisfied, whereby the interclade divergences were at least four times the maximum intraclade divergences (Birky *et al.* 2005).

Microplastics

Three particles were observed between the four specimens. One particle was a 649.648 μm long, dark fibre extracted from the juvenile from 6949 m (Fig. 3). FTIR analysis determined this fibre to be 83.74% similar to polyethylene terephthalate (PET). FTIR analysis resolved the second and third particles to be of biological nature, likely undigested material. Additionally, one cotton fibre (74.08% similar to cellulose) was found in the filter used as a blank during the specimen dissection. No particles were present in the procedural blanks.



FIGURE 3. Microfibre found within the hindgut of a *Eurythenes plasticus* sp. nov. individual from 6949 m in the Mariana Trench.

Systematics

Order Amphipoda Latreille, 1816

Superfamily Lysianassoidea Dana, 1849

Family Eurythenidae Stoddart & Lowry, 2004

Genus *Eurythenes* S. I. Smith in Scudder, 1882

***Eurythenes plasticus* sp. nov.** Weston

(Figs. 4–8)

Material Examined.

HOLOTYPE: Mature female, USNM 1615729, body length 48.1 mm.

PARATYPES: Mature male, USNM 1615732, GenBank (16S MT021437), (COI MT038070), body length 47.6 mm, Mariana Trench, Pacific Ocean (11.5911N, 144.84730E), cruise FK141109, station LH14, depth 6010 m. Immature female, USNM 1615733 GenBank (16S MT021438), (COI MT038071), body length 38.6 mm, Mariana Trench, Pacific Ocean (11.6071N, 144.8331E), cruise FK141109, station LH15, depth 6142 m. Juvenile, USNM XXXX3, body length 15.6 mm, same collection location as type locality.

PARAGENETYPE: Juvenile, GenBank (16S MT021439), (COI MT038072), body length 15.1 mm, same collection location as type locality.

NON-TYPE SPECIMENS: Three juveniles, body lengths 12.5, 13.5 & 15.7 mm, same collection location as type locality, USNM 1615731.

Type Locality. Mariana Trench, Pacific Ocean (12.64065N, 144.73796E), cruise FK141109, station WT02, depth 6865 m.

Etymology. The species names, *plasticus*, stems from Latin for plastic. This name speaks to the ubiquity of plastic pollution present in our oceans.

Diagnosis. Lateral cephalic lobe strongly produced, slightly triangular. Article 2 of mandibular palp narrow. Maxilliped inner plate with three to four apical protruding nodular setae. Gnathopod 1 subchelate, basis narrow (2.9x as long as wide), palm not protruding and weakly convex. Gnathopod 2 subchelate, coxa broad ventrally and weakly curved, palm convex. Pereopods 3 to 7 dactyli short. Pereopod 5 coxa bilobate and posterior lobe larger than anterior lobe. Epimeron 3 posteroventral corner subquadrate without small posteroventral tooth. Uropod 1 and 2 rami margins with spine-like setae. Dorsal carination with increasing degree on epimeron 1-3 and urosomite 1.

Description, based on holotype, female, USNM 1615729.

BODY (Figs. 4, 5, 6): surface smooth, without setae; urosomite 3 with an anterodorsal depression. *Oostegites* present on gnathopod 2 to pereopod 5, elongate but lacking setae. *Coxa gills* present on gnathopod 2 to pereopod 7. *Colour pattern* at time of recovery unknown.

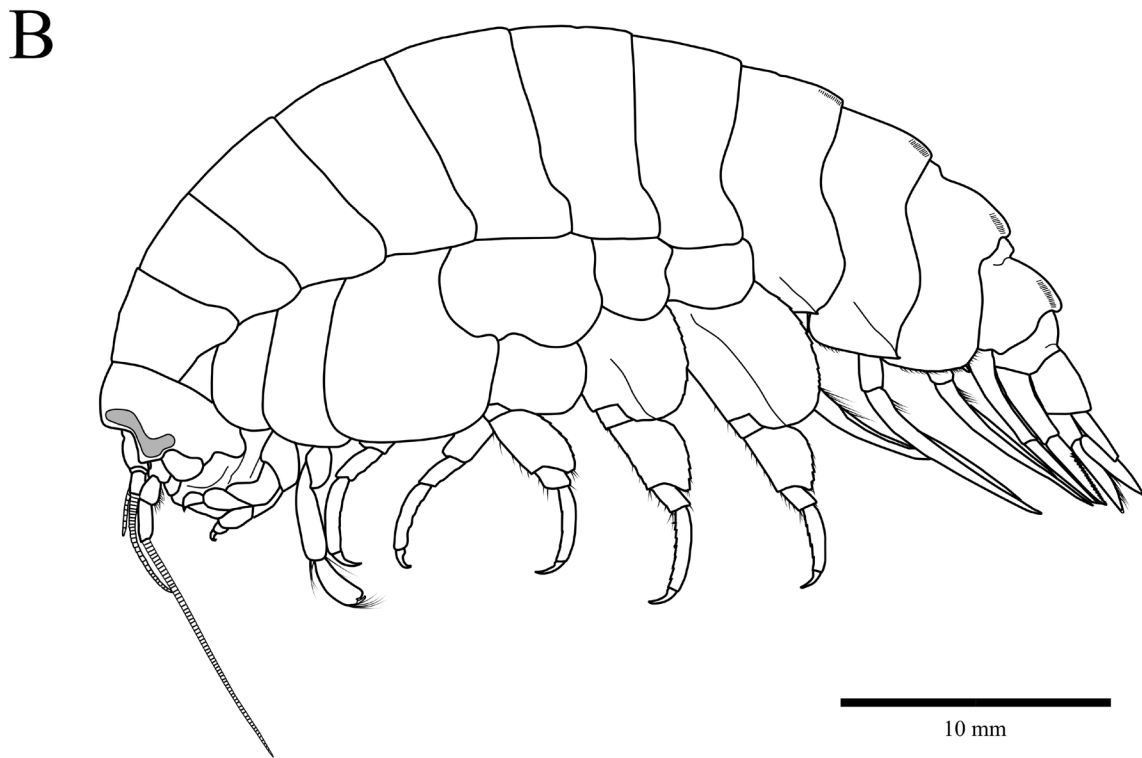


FIGURE 4. A, Photographs of specimens of *E. plasticus* sp. nov.: female holotype from 6865 m (A top; USNM 1615729), juvenile paratype from 6865 m (bottom left; USNM 1615730), male paratype from 6010 m (bottom right; USNM 1615732). B, *Eurythenes plasticus* sp. nov., mature female, holotype, USNM 1615729.

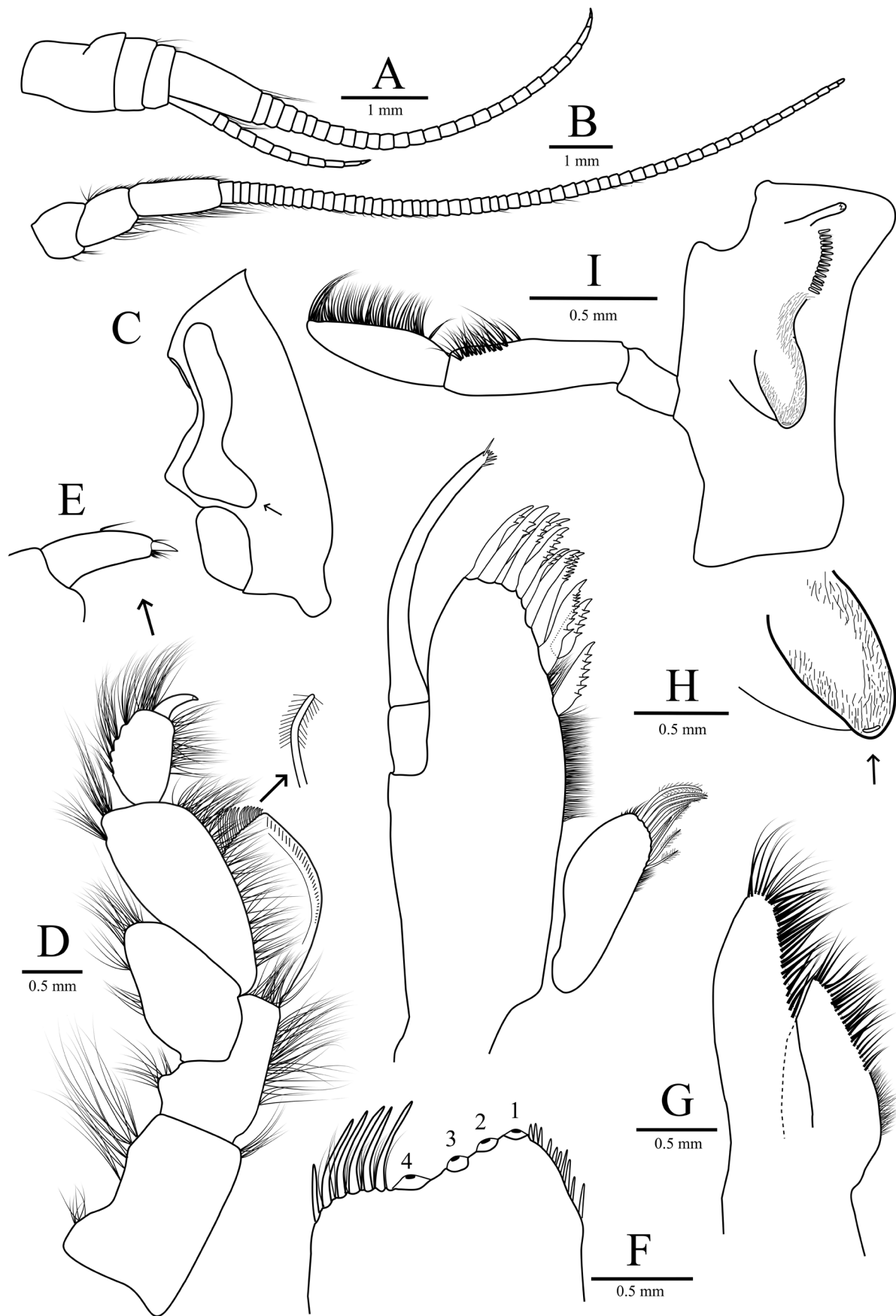


FIGURE 5. *Eurythenes plasticus* sp. nov. holotype (USNM 1615729). A, left antenna 1; B, left antenna 2; C, head; D, left maxilliped with inner plate removed; E, maxilliped dactylus; F, left maxilliped inner plate (medio-facial spines not shown); G, left maxilla 2; H, left maxilla 1 (palp not flattened); I, left mandible with molar insert.

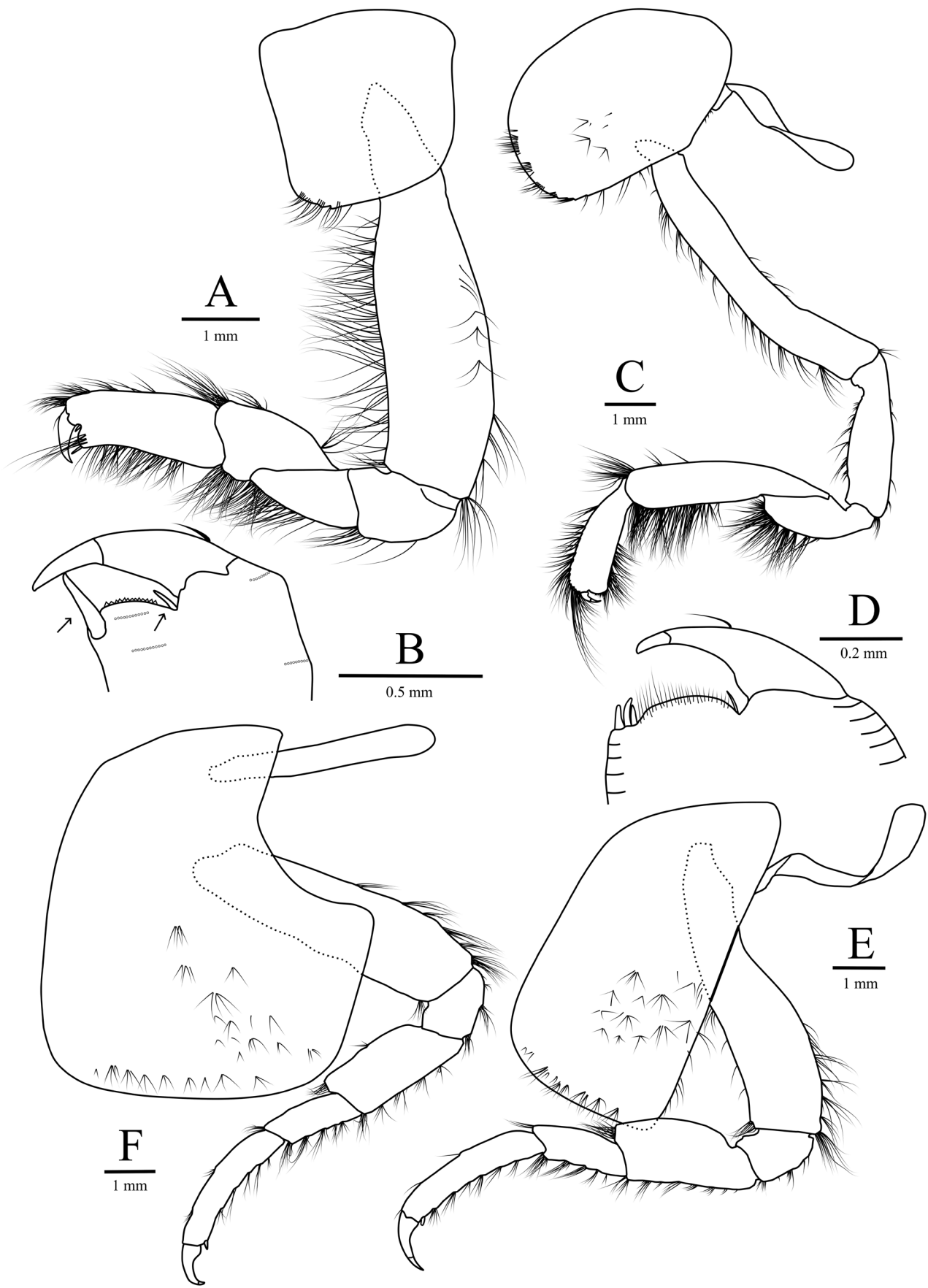


FIGURE 6. *Eurythenes plasticus* sp. nov. holotype (USNM 1615729). A, left gnathopod 1; B, chela of left gnathopod 1; C, left gnathopod 2; D, chela of left gnathopod 2; E, left pereopod 3; F, left pereopod 4.

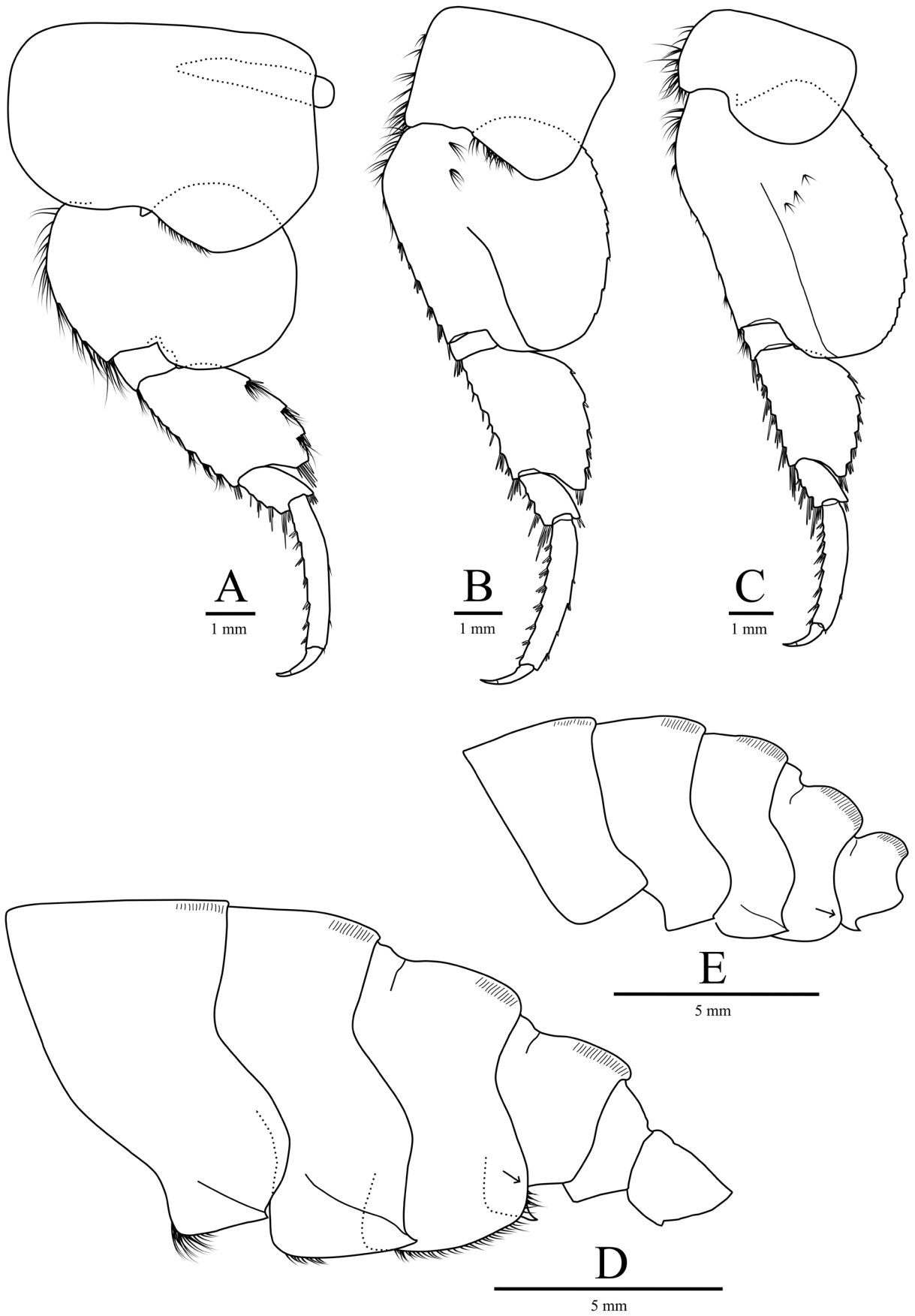


FIGURE 7. *Eurythenes plasticus* sp. nov. holotype (USNM 1615729). A, left pereopod 5; B, left pereopod 6; C, left pereopod 7; D, epimeron. *Eurythenes plasticus* sp. nov. paratype (USNM 1615730). E, epimeron.

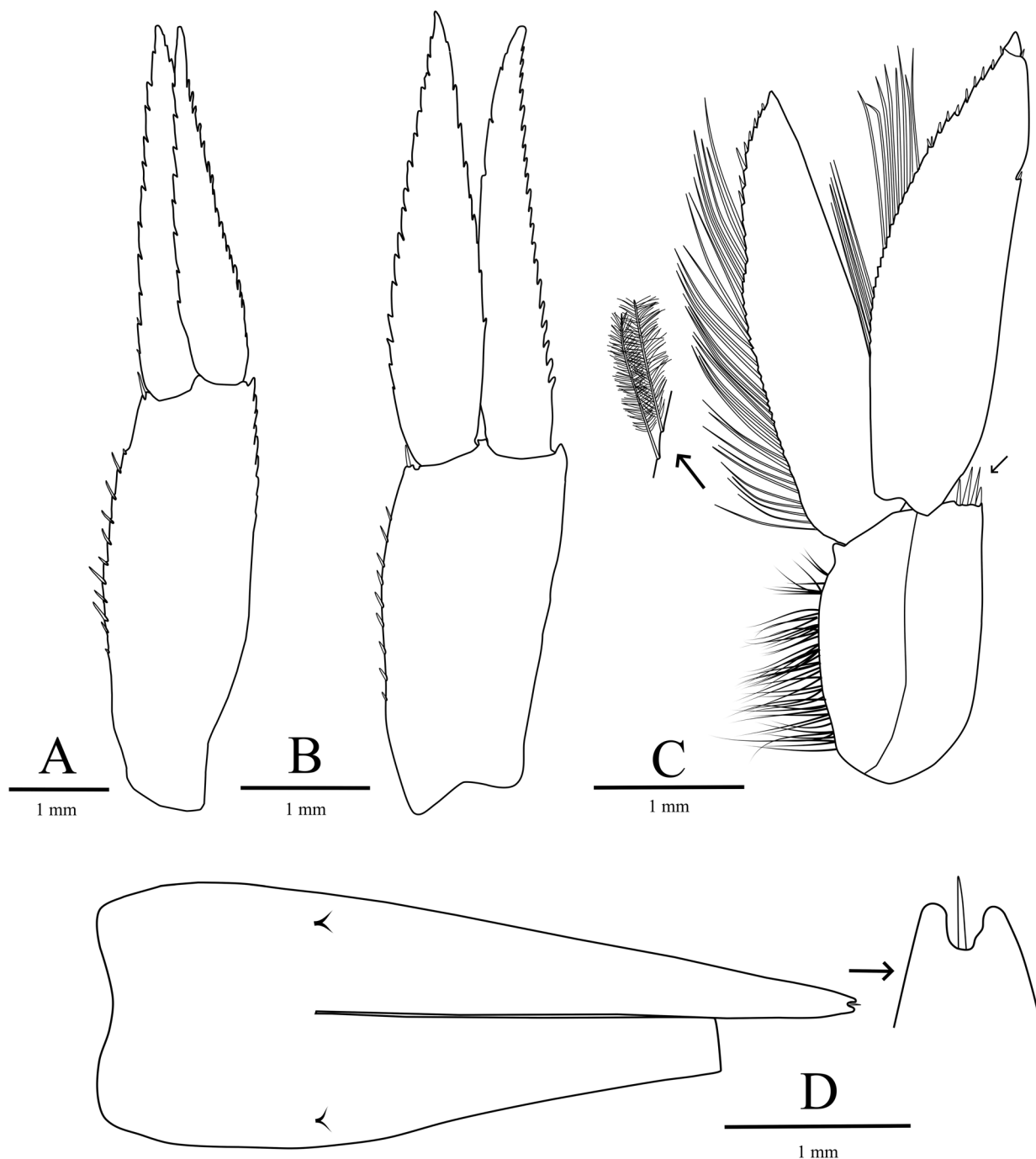


FIGURE 8. *Eurythenes plasticus* sp. nov. holotype (USNM 1615729). A, left uropod 1; B, left uropod 2; C, left uropod 3, D, telson with right distal margin insert.

HEAD (Fig. 5): rostrum absent; ventral corner of eye rounded and obliquely pointing backwards (Fig. 5C). *Antenna 1* short, 0.1x as long as body length; accessory flagellum 12-articulate; primary flagellum 28-articulate; callynophore well-developed; calceoli absent (Fig. 5A). *Antenna 2* medium length, 0.3x as long as body, 1.8x as long as antenna 1; flagellum 59-articulate; calceoli absent (Fig. 5B).

MOUTHPART BUNDLE (Fig. 5): *Mandible* left lacinia mobilis a long slender distally cuspidate robust seta; setal row left with 13 short, slender, robust setae; molar large, setose, vestigial distal triturating patch; palp article length ratio 1: 3.2: 2.6, article 2 posteriorly not expanded and distally not tapering, 3.4x as long as wide; article 3 blade-like (Fig. 5I). *Maxilla 1* inner plate with nine apical and sub-apical plumose setae; outer plate with an 8/3 setal crown arrangement; palp longer than outer plate, 2-articulate, seven sub-apical and apical setae with one being a flag

seta (Fig. 5H). *Maxilla 2* inner and outer plates broad, inner plate 0.6x shorter than outer plate (Fig. 5G). *Maxilliped* inner plate large, sub-rectangular, four apical protruding nodular setae; outer plate subovate, with 12 apical setose setae; palp large and well-developed; dactylus well-developed, unguis present, six small apical setae (Fig. 5D, F).

PEREON (Figs. 6, 7): *Gnathopod 1* coxa very weakly anteriorly concave, anteroventral margin with setae; palm crenulate, 0.4x as long as width of propodus, defined by one robust seta at base of palm and another robust seta at end of palm that is 2.6x longer; dactylus curved posteriorly, one long anterodistal seta, unguis present (Fig. 6A, B). *Gnathopod 2* subchelate, coxa obovate, broad ventrally and weakly curved; propodus elongate, not expanded distally, 6.1x as long as wide; propodus 2.7x as long as wide, moderately expanded distally; palm crenulate, distal end defined by three robust setae; dactylus not reaching palmar corner, curved posteriorly, unguis present, one long anterodistal seta (Fig. 6A, B). *Pereopod 3* coxa sub-rectangular, 2.0x as long as wide, setae on surface of coxa and along ventral and posterior margins; basis weakly expanded posteriorly, 2.7x as long as wide; merus expanded anteriorly, tuft of setae on anteroventral corner; propodus 4.8x as long as wide; dactylus short, 0.4x as long as propodus, unguis present (Fig. 6C). *Pereopod 4* coxa broad, 1.2x as long as wide, 1.1x length of coxa 3, junction between anterior and ventral border bluntly angular (sub-rectangular), ventral border straight, posteroventral border straight and weakly oblique; leg almost identical with pereopod 3 (Fig. 6D). *Pereopod 5* coxa bilobate, posterior lobe 1.3x longer and 1.6x wider than anterior lobe, ventral border of posterior lobe sub-triangular; basis expanded posteriorly, posterior margin smooth; merus broadly expanded posteriorly, 1.5x as long as wide, curved posterior margin; propodus slender, 6.2x as long as wide, seven groups of robust setae on the anterior margin; dactylus short, 0.4x as long as propodus, unguis present (Fig. 7A). *Pereopod 6* coxa subquadrate, posterior margin weakly bilobate or weakly concave; basis expanded posteriorly, posterior margin distinctly crenate; merus broadly expanded posteriorly, 1.7x as long as wide, convex posterior margin; propodus slender, 5.9x as long as wide, eight groups of robust setae on the anterior margin; dactylus slender, short, 0.3x as long as propodus, unguis present (Fig. 7B). *Pereopod 7* coxa sub-rectangular; basis with posterior border crenulate and strongly expanded, distal lobe moderately protruding; merus broadly expanded posteriorly, 1.6x as long as wide, convex posterior margin; propodus with normal stoutness, 5.6x as long as wide, eight groups of robust setae on the anterior margin; dactylus slender, short, 0.3x as long as propodus, unguis present (Fig. 7C).

PLEON AND UROSOME (Figs. 7, 8): *Epimeron 1* anteroventral corner rounded with long slender setae; posteroventral corner produced into a small tooth. *Epimeron 2* anteroventral margin lined with short fine setae; posteroventral corner produced into a strong tooth. *Epimeron 3* ventral margin lined with long fine setae, weakly curved (Fig. 7D). *Urosomite 1* with anterodorsal notch (Fig. 7D). *Uropod 1* peduncle with one apicomedial setae; inner ramus subequal in length to outer ramus; outer ramus 0.85x as long as peduncle; outer ramus with 18 lateral and eight medial spine-like setae; inner ramus with 20 lateral and 11 medial spine-like setae (Fig. 8A). *Uropod 2* peduncle with one apicomedial setae; inner ramus subequal in length (0.9x) to outer ramus; outer ramus subequal in length to peduncle outer ramus with 20 lateral and three medial spine-like setae; inner ramus with seven lateral and 16 medial spine-like setae (Fig. 8B). *Uropod 3* inner ramus subequal in length to article 1 of outer ramus; article 2 of outer rami short, 0.05x length of article 1; setae of distolateral angle of peduncle of normal length and stoutness; medial margins of both rami with plumose setae (Fig. 8C). *Telson* 70% cleft, pair of apical setae on each lobe parallel with beginning of cleft, distal margin with a single apical seta on right lobe, distal end of left lobe missing (Fig. 8D).

Variations. As with other species of *Eurythenes*, there appears to be very little sexual dimorphism. In part, this could be limited to having a single male specimen. The mature male paratype (USNM 1615732) has calceoli present on both antenna 1 and antenna 2. Both antennae are shorter than the holotype with antenna 1 accessory flagellum being 10-articulate, antenna 1 25-articulate, and antenna 2 54-articulate. Additionally, the maxilliped inner plate of the male paratype has three apical protruding nodular setae, specifically lacking the third setae present on the holotype (Fig. 5F). There were differences present in the juvenile paratype (USNM 1615730) that included typical cohort differences among *Eurythenes*, such as fewer setae on pereopods and uropods and reduced articulation on antennae (antenna 1 accessory flagellum 7-articulate, antenna 1 15-articulate, and antenna 2 38-articulate). In addition, the juvenile paratype had more pronounced and raised dorsal carination than on the adults (Fig. 7E). This difference was present among all the juvenile specimens observed.

Differential Diagnosis. As highlighted in d'Udekem d'Acoz & Havermans (2015), the morphological characteristics that separate and define the species within the *gryllus*-complex are hard to observe and should be used with caution. *Eurythenes plasticus* sp. nov. is a member of the *gryllus*-complex morphologically and genetically. Nevertheless, there is a combination of characters that are unique to *E. plasticus* sp. nov. and allow it to be distinguished

from the morphologically similar species *E. andhakarae*, *E. magellanicus*, and *E. aequilatus*. The most distinctive characteristics are the robust, spine-like setae on rami of uropod 1 and 2 (Fig. 8A, B) and the lobes of pereopod 5 coxa (Fig. 7A), here being unequal, which is novel within *Eurythenes*. *Eurythenes plasticus* sp. nov. can be differentiated from *E. andhakarae* with article 2 of the mandible palp being narrow (instead of expanded), four protruding nodular spines on the inner plate of the maxilliped (versus three non-protruding), and straight ventral border of coxa 4 (opposed to curved). *Eurythenes plasticus* sp. nov. can be separated from *E. magellanicus* with a long gnathopod 1 palm (instead of short), a straight ventral border of coxa 4 (opposed to curved), a subquadrate posteroventral corner in epimeron 3 (instead of bearing a small tooth), and the rami of uropod 1 and 2 being subequal (opposed to uropod 2 outer ramus being shorter than inner ramus and uropod 1 outer ramus being longer than inner ramus). *Eurythenes plasticus* sp. nov. can also be distinguished from *E. aequilatus* by its eyes with a variable width (opposed to constant width), the outer plate of maxilla 1 with 8/3 crown arrangement (instead of 9/3 arrangement), and a long gnathopod 1 palm (instead of short).

Habitat, Distribution and Biology. *Eurythenes plasticus* sp. nov. was collected from the upper hadal depths of the Mariana Trench, between 6010 and 6949 m. Similar to sister species within the genus, *E. plasticus* sp. nov. is a benthic scavenger, as individuals of multiple cohorts entered the baited traps. *Eurythenes plasticus* sp. nov. is a member of a wider scavenging amphipod community comprised of *A. gigantea*, *Bathycallisoma schellenbergi* (Birstein & Vinogradov, 1958), *Hirondellea dubia* Dahl, 1959, *H. gigas*, *Paralicella caperesca* Shulenberg & Barnard, 1976, *Paralicella tenuipes* Chevreux, 1908, and *Valettietta anacantha* (Birstein & Vinogradov, 1963), which were concurrently recovered in the traps (data unpublished).

Discussion

The salient finding of this study is the paired molecular and morphological identification approaches provided congruent evidence that *E. plasticus* sp. nov. represents an undescribed species within *Eurythenes*. Further, as a scavenger at upper hadal depths (6010 – 6949 m) in the Mariana Trench, *E. plasticus* sp. nov. is not exempt from ingesting microplastics that are bioavailable within the hadal zone.

In comparison to described *Eurythenes* species, *E. plasticus* sp. nov. was placed as part of the *gryllus*-complex and most closely related to the abyssal *E. magellanicus* (Fig. 2). The bPTP analysis of COI and both K2P analyses delineated *E. plasticus* sp. nov. to be a distinctive lineage, and these methods aligned with previous studies that detected cryptic speciation within the *gryllus*-complex (Havermans *et al.* 2013; Eustace *et al.* 2016; Narahara-Nakano *et al.* 2017). The 16S phylogeny specifically showed *E. plasticus* sp. nov. to be nearly identical to Eg7 (Fig. 2A; France & Kocher 1996; Havermans *et al.* 2013). This *Eurythenes* sp. was a singleton recovered from abyssal depths at the Horizon Guyot seamount, Pacific Ocean, and it was collected along with another *Eurythenes* sp. from the divergent Eg9 clade (Havermans *et al.* 2013). Confidence in the identification of Eg7 would be further strengthened with additional genetic or morphological data.

The morphological variation seen in *E. plasticus* sp. nov., such as an uneven coxa 5 lobe and lack of a tooth on the posteroventral corner of epimeron 3, supported the phylogenetic evidence as an undescribed lineage. Consistent with previous studies, these morphological characteristics should be used with caution, as some are difficult to discern objectively. Additional specimens, like from the Eg7 clade, may reveal phenotypic plasticity in the characteristics observed in this morphological study (d'Udekem d'Acoz & Havermans 2015). Continued application of a combined molecular and morphological approaches in future studies is likely to reveal further species diversity within the *gryllus*-complex.

The discovery of *E. plasticus* sp. nov. continues to align with the pattern *Eurythenes* that the geographic and bathymetric species distributions are complex (Havermans 2016). With the Eg7 singleton, the geographic range of *E. plasticus* sp. nov. thus far appears to be restricted to the Central Pacific Ocean. Across that ocean basin, *E. plasticus* sp. nov. has broad bathymetric range, ~3000 m. While it is common among *Eurythenes* to be found only in a single ocean basin and have a wide vertical distribution (Eustace *et al.* 2016; Havermans 2016), it is less common to span across the abyssal and hadal zones. Although, this is not unique, as it has been documented in other amphipods, such as *A. gigantea* (Jamieson *et al.* 2013). A species needs to be able to cope at the cellular, reproductive, and physiological levels in both the stable abyssal (Smith *et al.* 2008) and the dynamic hadal environments (Jamieson 2015; Downing *et al.* 2018). Yet, it was curious that during the present study, *E. plasticus* sp. nov. was only collected from upper hadal depths, despite amphipods being captured at shallower and deeper depths (43 additional deployments 4506 to 10545 m; data unpublished). This highlights that the distribution of *E. plasticus* sp. nov. is a patchwork. Further work and sampling will be required to understand the conditions that support the presence of this species.

The finding of a microplastic fibre in the hindgut of a juvenile was not unexpected. Deep-sea scavenging amphipods, as an adaptation to their food limited environment, indiscriminately consume carrion (Blankenship & Levin 2007) and are known to inadvertently ingest microfibrils present in the carrion and sediment (Jamieson *et al.* 2019). The detection of a microplastic adds to the number of hadal scavenging amphipods, including adult specimens of *H. gigas* from the Mariana Trench and *Eurythenes* sp. 'hadal' the Peru-Chile Trench (Jamieson *et al.* 2019), which have been found to have consumed plastic microfibers. Microplastic consumption by a juvenile indicates that scavenging amphipods are potentially ingesting microplastics throughout their life, which could pose acute and chronic health effects. While the ecotoxicological impacts of microplastic exposure has yet to be investigated on deep-sea amphipods, early work on other Malacostraca indicates that the ingestion of polypropylene fibres by the sand crab, *Emerita analoga*, increases adult mortality and decreases in retention of egg clutches (Horn *et al.* 2019).

This study adds to the growing body of literature on marine organisms ingesting plastic and microfibers (Beseling *et al.* 2015; Lusher *et al.* 2015; Bellas *et al.* 2016; Alomar & Deudero 2017). The microplastic found in the hindgut of *E. plasticus* sp. nov. was most similar to PET, which is one of the top five most prevalent synthetic plastic polymers produced and discarded globally (Geyer *et al.* 2017). Without substantial global changes to the life cycle of plastic, from reducing the rate of plastic production to improving waste management (Forrest *et al.* 2019), plastics and microfibers will continue to be transported to the deep sea and be ubiquitous in the hadal food chain for the foreseeable future.

Acknowledgments

We extend thanks to Eva Stewart and Jenny Wainwright (Newcastle University) for their dissertation work that laid the foundation for this description. We are grateful to Drs Shannon Flynn (Newcastle University) and Renate Matzke-Karasz (Ludwig-Maximilians-Universität München) for their constructive comments on manuscript drafts. We thank the collections staff at the Smithsonian Institution National Museum of Natural History for their efficiency and generosity in curating the type material. We sincerely thank the HADES-M Chief Scientist Dr Jeffrey Drazen (University of Hawai'i at Manoa) and the Captain and crew of the *R/V Falkor* (FK141109) for their work to collect the specimens. We thank the National Oceanic and Atmospheric Administration (NOAA), National Marine Fisheries Service (NMFS) Pacific Islands Fisheries Science Center, the Pacific Islands Regional Office, the Marine National Monuments Program, and Eric Breuer (NOAA/NMFS) for their collaboration with HADES-M. Thank you to the reviewer for their constructive comments that improved the manuscript.

Funding

HADES-M and the expedition cruise FK141109 on the *R/V Falkor* was supported by the National Science Foundation Grant OCE #1130712, the Schmidt Ocean Institute, and the Marine Alliance for Science and Technology for Scotland. The molecular analysis was funded by Newcastle University, UK through internal support. The microplastics analysis and laboratory was funded by the European Maritime and Fisheries Fund (EMFF), under grant number ENG2954. The description was supported by the World Wildlife Fund (WWF).

References

- Alomar, C. & Deudero, S. (2017) Evidence of microplastic ingestion in the shark *Galeus melastomus* Rafinesque, 1810 in the continental shelf off the western Mediterranean Sea. *Environmental Pollution*, 223, 223–229.
<https://doi.org/10.1016/j.envpol.2017.01.015>
- Barnard, J.L. (1962) South Atlantic abyssal amphipods collected by R.V. Vema. In: Barnard, J.L., Menzies, R.J. & Băcescu, M.C. (Eds.), *Abyssal Crustacea*. Columbia University Press, New York and London, pp. 1–78.
- Bellas, J., Martínez-Armentál, J., Martínez-Cámara, A., Besada, V. & Martínez-Gómez, C. (2016) Ingestion of microplastics by demersal fish from the Spanish Atlantic and Mediterranean coasts. *Marine Pollution Bulletin*, 109 (1), 55–60.
<https://doi.org/10.1016/j.marpolbul.2016.06.026>
- Besseling, E., Foekema, E.M., Van Franeker, J.A., Leopold, M.F., Kühn, S., Bravo Rebolledo, E.L., Heße, E., Mielke, L.J.I.J., Ijzer, J., Kamminga, P. & Koelmans, A.A. (2015) Microplastic in a macro filter feeder: Humpback whale *Megaptera no-*

- vaeangliae*. *Marine Pollution Bulletin*, 95 (1), 248–252.
<https://doi.org/10.1016/j.marpolbul.2015.04.007>
- Birky, C., Wolf, C., Maughan, H., Herbertson, L. & Henry, E. (2005) Speciation and selection without sex. *Hydrobiologia*, 546 (1), 29–45.
<https://doi.org/10.1007/s10750-005-4097-2>
- Blankenship, L.E. & Levin, L.A. (2007) Extreme food webs: Foraging strategies and diets of scavenging amphipods from the ocean's deepest 5 kilometers. *Limnology and Oceanography*, 52 (4), 1685–1697.
- Brandt, A., Błażewicz-Paszkowycz, M., Bamber, R.N., Mühlenhardt-Siegel, U., Malyutina, M.V., Kaiser, S., De Broyer, C. & Havermans, C. (2012) Are there widespread peracarid species in the deep sea (Crustacea: Malacostraca)? *Polish Polar Research*, 33 (2), 139–162.
<https://doi.org/10.2478/v10183-012-0012-5>
- Charette, M.A. & Smith, W.H.F. (2010) The volume of the Earth's ocean. *Oceanography*, 23 (2), 112–114.
<https://doi.org/10.5670/oceanog.2010.51>
- Chevreaux, E. (1905) Description d'un amphipode (*Katius obesus*, nov. gen. et sp.), suivie d'une liste des amphipodes de la tribu des Gammarina ramenés par le filet à grand ouverture pendant la dernière campagne de la *Princesse-Alice* en 1904. *Bulletin du Musée océanographique de Monaco*, 35, 1–7.
- Chiba, S., Saito, H., Fletcher, R., Yogi, T., Kayo, M., Miyagi, S., Ogido, M. & Fujikura, K. (2018) Human footprint in the abyss: 30 year records of deep-sea plastic debris. *Marine Policy*, 96, 204–212.
<https://doi.org/10.1016/j.marpol.2018.03.022>
- Coleman, C.O. (2003) “Digital inking”: How to make perfect line drawings on computers. *Organisms Diversity & Evolution*, 3, 1–14.
- Coleman, C.O. (2009) Drawing setae the digital way. *Zoosystems Evolution*, 85 (2), 305–310.
<https://doi.org/10.1002/zoos.200900008>
- Cornils, A. & Held, C. (2014) Evidence of cryptic and pseudocryptic speciation in the *Paracalanus parvus* species complex (Crustacea, Copepoda, Calanoida). *Frontiers in Zoology*, 11 (1), 19.
<https://doi.org/10.1186/1742-9994-11-19>
- Downing, A.B., Wallace, G.T. & Yancey, P.H. (2018) Organic osmolytes of amphipods from littoral to hadal zones: Increases with depth in trimethylamine N-oxide, scyllo-inositol and other potential pressure counteractants. *DeepSea Research Part I: Oceanographic Research Papers*, 138, 1–10.
<https://doi.org/10.1016/j.dsr.2018.05.008>
- d'Udekem d'Acoz, C. & Havermans, C. (2015) Contribution to the systematics of the genus *Eurythenes* S. I. Smith in Scudder, 1882 (Crustacea: Amphipoda: Lysianassoidea: Eurythenidae). *Zootaxa*, 3971 (1), 1–80.
<https://doi.org/10.11646/zootaxa.3971.1.1>
- Drummond, A.J., Ho, S.Y.W., Phillips, M.J. & Rambaut, A. (2006) Relaxed phylogenetics and dating with confidence. *Public Library of Science Biology*, 4, e88.
<https://doi.org/10.1371/journal.pbio.0040088>
- Drummond, A.J., Suchard, M.A., Xie, D. & Rambaut, A. (2012) Bayesian phylogenetics with BEAUti and the BEAST 1.7. *Molecular Biology and Evolution*, 29 (8), 1969–1973.
<https://doi.org/10.1093/molbev/mss075>
- Escobar-Briones, E., Nájera-Hillman, E. & Álvarez, F. (2010) Unique 16S rRNA sequences of *Eurythenes gryllus* (Crustacea: Amphipoda: Lysianassidae) from the Gulf of Mexico abyssal plain. *Revista Mexicana de Biodiversidad*, 81, 177–185.
- Eustace, R.M., Kilgallen, N.M., Ritchie, H., Piertney, S.B. & Jamieson, A.J. (2016) Morphological and ontogenetic stratification of abyssal and hadal *Eurythenes gryllus sensu lato* (Amphipoda: Lysianassidae) from the Peru-Chile Trench. *Deep Sea Research I: Oceanographic Research Papers*, 109, 91–98.
<https://doi.org/10.1016/j.dsr.2015.11.005>
- Foekema, E.M., De Gruijter, C., Mergia, M.T., van Franeker, J.A., Murk, A.J. & Koelmans, A.A. (2013) Plastic in North Sea fish. *Environmental Science & Technology*, 47 (15), 8818–8824.
<https://doi.org/10.1021/es400931b>
- Folmer, O., Black, M., Hoeh, W., Lutz, R. & Vrijenhoek, R. (1994) DNA primers for amplification of mitochondrial cytochrome c oxidase subunit I from diverse metazoan invertebrates. *Molecular Marine Biology and Biotechnology*, 3, 294–299.
- Forrest, A., Giacobazzi, L., Dunlop, S., Reisser, J., Tickler, D., Jamieson, A.J. & Meeuwig, J.J. (2019) Eliminating plastic pollution: How a voluntary contribution from industry will drive the circular plastics economy. *Frontiers in Marine Science*, 6: 627.
<https://doi.org/10.3389/fmars.2019.00627>
- France, S.C. & Kocher, T.D. (1996) Geographic and bathymetric patterns of mitochondrial 16S rRNA sequence divergence amount deep-sea amphipods, *Eurythenes gryllus*. *Marine Biology*, 126 (4), 633–643.
- Fujii, T., Kilgallen, N.M., Rowden, A.A. & Jamieson, A.J. (2013) Deep-sea amphipod community structure across abyssal to hadal depths in the Peru-Chile and Kermadec trenches. *Marine Ecology Progress Series*, 492, 125–138.
<https://doi.org/10.3354/meps10489>
- Garlitska, L., Neretina, T., Schepetov, D., Mugué N.M., De Troch, M., Baguley, J.G., & Azovsky, A. (2012) Cryptic diversity of the ‘cosmopolitan’ harpacticoid copepod *Nannopus palustris*: genetic and morphological evidence. *Molecular Ecology*,

- 21 (21), 5336–5347.
<https://doi.org/10.1111/mec.12016>
- GEBCO (2015) GEBCO_2014Grid [WWWDocument]. Gen.Bathymetr.ChartOcean. (URL) Available from: http://www.gebco.net/data_and_products/gridded_bathymetry_data/gebco_30_second_grid/ (accessed 05.11.19)
- Geyer, R., Jambeck, J.R. & Lavender Law, K. (2017) Production, use, and fate of all plastic ever made. *Science Advances*, 3 (7), e1700782.
<https://doi.org/10.1126/sciadv.1700782>
- Hargrave, B.T. (1985) Feeding rates of abyssal scavenging amphipods (*Eurythenes gryllus*) determined *in situ* by time-lapse photography. *Deep Sea Research Part A. Oceanographic Research Papers*, 32 (4), 443–450.
[https://doi.org/10.1016/0198-0149\(85\)90090-1](https://doi.org/10.1016/0198-0149(85)90090-1)
- Hasegawa, M., Kishino, H. & Yano, T. (1985) Dating the human-ape splitting by a molecular clock of mitochondrial DNA. *Journal of Molecular Evolution*, 22 (2), 160–174.
- Havermans, C., Sonet, G., d’Udekem d’Acoz, C., Nagy, Z.T., Martin, P., Brix, S., Riehl, T., Agrawal, S. & Held, C. (2013) Genetic and morphological divergences in the cosmopolitan deep-sea amphipod *Eurythenes gryllus* reveal a diverse abyss and bipolar species. *Public Library of Science One*, 8 (9), e74218.
<https://doi.org/10.1371/journal.pone.0074218>
- Havermans, C. (2016) Have we so far only seen the tip of the iceberg? Exploring species diversity and distribution of the giant amphipod *Eurythenes*. *Biodiversity*, 17 (1–2), 12–25.
<https://doi.org/10.1080/14888386.2016.1172257>
- Havermans, C. & Smetacek, V. (2018) Bottom-up and top-down triggers of diversification: A new look at the evolutionary ecology of scavenging amphipods in the deep sea. *Progress in Oceanography*, 164, 37–51.
<https://doi.org/10.1016/j.pocean.2018.04.008>
- Hessler, R.R., Ingram, C.L., Yayanos, A.A. & Burnett, B.R. (1978) Scavenging amphipods from the floor of the Philippine Trench. *Deep Sea Research*, 25 (11), 1029–1047.
[https://doi.org/10.1016/0146-6291\(78\)90585-4](https://doi.org/10.1016/0146-6291(78)90585-4)
- Horn, D., Granek, E.F. & Steele, C.L. (2019) Effects of environmentally relevant concentrations of microplastic fibers on Pacific mole crab (*Emerita analoga*) mortality and reproduction. *Limnology and Oceanography Letters*.
<https://doi.org/10.1002/lo2.10137>
- Horton, T. & Thurston, M.H. (2014) A revision of the bathyal and abyssal necrophage genus *Cyclocaris* Stebbing, 1888 (Crustacea: Amphipoda: Cyclocaridae) with the addition of two new species from the Atlantic Ocean. *Zootaxa*, 3796 (3), 507–527.
<http://dx.doi.org/10.11646/zootaxa.3796.3.6>
- Ingram, C.L. & Hessler, R.R. (1983) Distribution and behavior of scavenging amphipods from the central North Pacific. *Deep Sea Research Part A. Oceanographic Research Papers*, 30 (7), 683–706.
[http://dx.doi.org/10.1016/0198-0149\(83\)90017-1](http://dx.doi.org/10.1016/0198-0149(83)90017-1)
- Ingram, C.L. & Hessler, R.R. (1987) Population biology of the deep-sea amphipod *Eurythenes gryllus*: inferences from instar analyses. *Deep Sea Research Part A. Oceanographic Research Papers*, 34 (12), 1889–1910.
- Jamieson, A.J. (2015) The hadal zone: Life in the deepest oceans, 1st ed. Cambridge University Press, Cambridge, UK.
- Jamieson, A.J., Lacey, N.C., Lörz, A.N., Rowden, A.A. & Piertney S.B. (2013) The supergiant amphipod *Alicella gigantea* (Crustacea: Alicellidae) from hadal depths in the Kermadec Trench, SW Pacific Ocean. *Deep Sea Research II: Topical Studies in Oceanography*, 92, 107–113.
<https://doi.org/10.1016/j.dsr2.2012.12.002>
- Jamieson, A.J., Brooks, L.S.R., Reid, W.D.K., Piertney, S.B., Narayanaswamy, B.E., & Linley, T.D. (2019) Microplastics and synthetic particles ingested by deep-sea amphipods in six of the deepest marine ecosystems on Earth. *Royal Society Open Science*, 6 (2), 180667.
<http://dx.doi.org/10.1098/rsos.180667>
- Katoh, K., Rozewicki, J. & Yamada, K.D. (2019) MAFFTA online service: multiple sequence alignment, interactive sequence choice and visualization. *Briefings in Bioinformatics*, 20 (4), 1160–1166.
<https://doi.org/10.1093/bib/bbx108>
- Kimura, M. (1980) A simple method for estimating evolutionary rates of base substitutions through comparative studies of nucleotide sequences. *Journal of Molecular Ecology*, 16, 111–120.
- King, N.J & Priede, I.G. (2008) *Coryphaenoides armatus*, the abyssal grenadier global distribution, abundance, and ecology as determined by baited landers. *American Fisheries Society Symposium*, 63, 139–161.
- Kumar, S., Stecher, G. & Tamura, K. (2016) MEGA7: Molecular Evolutionary Genetics Analysis version 7.0 for bigger datasets. *Molecular Biology and Evolution*, 33 (7), 1870–1874.
<https://doi.org/10.1093/molbev/msw054>
- Lichtenstein, H. (1822). §. 30 [Crustacea]. In: Mandt, M.G. (Ed.), *Observationes in historiam naturalem et anatomiam comparatam in itinere Groenlandico factae. Dissertatio inauguralis quam consensu et auctoritate gratiosi medicorum ordinis in universitate literaria berolinensium iutsummi in medicina et chirurgia honores rite sibiconcedantur die XXII. M. Iulii A. MDCCCXXIII.L.Q.S., publice defendet auctor Martinus Gulielmus Mandt Beyenburgensis. Opponentibus: J.Th. v. Brandt Med. Cd., J. Ollenroth Med. Cd., E. Gabler Med. Cd.; FormisBrueschckianis, Berlin, pp.31–37.*
- Lusher, A.L., O’Donnell, C., Officer, R. & O’Connor, I. (2016) Microplastic interactions with North Atlantic mesopelagic fish.

- ICES *Journal of Marine Science*, 73, 1214–1225.
<https://doi.org/10.1093/icesjms/fsv241>
- Madsen, F.J. (1961) On the zoogeography and origin of the abyssal fauna, in view of the knowledge of the Porcellanasteridae. *Galathea Rep*, 4, 177–218.
- Markmann, M. & Tautz, D. (2005) Reverse taxonomy: an approach towards determining the diversity of meiobenthic organisms based on ribosomal RNA signature sequences. *Philosophical Transactions of the Royal Society B: Biological Sciences*, 360 (1462), 1917–1924.
<https://doi.org/10.1098/rstb.2005.1723>
- Milne Edwards, H. (1848) Sur un crustacé amphipode, remarquable par sa grandetaille. *Annales des Sciences Naturelles*, 3 (9), 398.
- Murphy, F., Ewins, C., Carbonnier, F. & Quinn, B. (2016) Waste water treatment works (WwTW) as a source of microplastics in the aquatic environment. *Environmental Science & Technology*, 50 (11), 5800–5808.
<https://doi.org/10.1021/acs.est.5b05416>
- Narahara-Nakano, Y., Nakano, T. & Tomikawa, K. (2018) Deep-sea amphipod genus *Eurythenes* from Japan, with a description of a new *Eurythenes* species from off Hokkaido (Crustacea: Amphipoda: Lysianassoidea). *Marine Biodiversity*, 48 (1), 603–620.
<https://doi.org/10.1007/s12526-017-0758-4>
- Palumbi, S., Martin, A. & Romano, S. (2002) The simple fool's guide to PCR, version 2.0. Department Zoology, University of Hawaii.
- Palumbi, S.R. (1994) Genetic divergence, reproductive isolation, and marine speciation. *Annual Review of Ecology and Systematics*, 25, 547–572.
<https://doi.org/10.1146/annurev.es.25.110194.002555>
- Peng, G., Bellerby, R., Zhang, F., Sun, X. & Li, D. (2020) The ocean's ultimate trashcan: Hadal trenches as major depositories for plastic pollution. *Water Research*, 168, 115121.
<https://doi.org/10.1016/j.watres.2019.115121>
- Peng, X., Chen, M., Chen, S., Dasgupta, S., Xu, H., Ta, K., Du, M., Li, J., Guo, Z. & Bai, S. (2018) Microplastics contaminate the deepest part of the world's ocean. *Geochemical Perspective Letters*, 9, 1–5.
<https://doi.org/10.7185/geochemlet.1829>
- Rambaut, A., Drummond, A.J., Xie, D., Baele, G. & Suchard, M.A. (2018) Posterior summarisation in Bayesian phylogenetics using Tracer 1.7. *Systematic Biology*, syy032.
<https://doi.org/10.1093/sysbio/syy032>
- Ritchie, H., Jamieson, A.J. & Piertney, S.B. (2015) Phylogenetic relationships among hadal amphipods of the Superfamily Lysianassoidea: Implications for taxonomy and biogeography. *DeepSea Research I: Oceanographic Research Papers*, 105, 119–131.
<https://doi.org/10.1016/j.dsr.2015.08.014>
- Ritchie, H., Jamieson, A.J. & Piertney, S.B. (2017) Genome size variation in deep-sea amphipods. *Royal Society Open Science*, 4, 170862.
<http://dx.doi.org/10.1098/rsos.170862>
- Saunders, P. (1981) Practical conversion of pressure to depth. *Journal of Physical Oceanography*, 11, 573–574.
- Schliep, K., Potts, A.J., Morrison, D.A. & Grimm, G.W. (2017) Intertwining phylogenetic trees and networks. *Methods in Ecology and Evolution*, 8, 1212–1220.
<https://doi.org/10.1111/2041-210X.12760>
- Schlining, K., von Thun, S., Kuhn, L., Schlining, B., Lundsten, L., Jacobsen Stout, N., Chaney, L. & Connor, J. (2013) Debris in the deep: Using a 22-year video annotation database to survey marine litter in Monterey Canyon, central California, USA. *Deep Sea Research I: Oceanographic Research Papers*, 79, 96–105.
<http://dx.doi.org/10.1016/j.dsr.2013.05.006>
- Smith, S.I. (1882) *Eurythenes* Lillgeborg. In: Scudder, S.H. (Ed.), *Zoologicus*, N., 1882. An alphabetical list of all generic names that have been employed by naturalists for recent and fossil animals from the earliest times to the close of the year 1879. 1. *Supplemental list of Genera in Zoology*. *Washington*, 21 (1), 376.
- Smith, C.R., De Leo, F.C., Bernardino, A.F., Sweetman, A.K. & Arbizu, P.M. (2008) Abyssal food limitation, ecosystem structure and climate change. *Trends in Ecology & Evolution*, 23 (9), 518–528.
<https://doi.org/10.1016/j.tree.2008.05.002>
- Stoddart, H.E. & Lowry, J.K. (2004) The deep-sea lysianassoid genus *Eurythenes* (Crustacea, Amphipoda, Eurytheneidae n. fam.). *Zoosystema*, 26 (3), 425–468.
- Taylor, M.L., Gwinnett, C., Robinson, L.F. & Woodall, L.C. (2016) Plastic microfiber ingestion by deep-sea organisms. *Scientific Reports*, 6, 33997.
<https://doi.org/10.1038/srep33997>
- Thurston, M.H., Petrillo, M. & Della Croce, N. (2002) Population structure of the necrophagous amphipod *Eurythenes gryllus* (Amphipoda: Gammaridae) from the Atacama Trench (south-east Pacific Ocean). *Journal of the Marine Biological Association of the United Kingdom*, 82, 205–211.
<https://doi.org/10.1017/S0025315402005374>

- Wesch, C., Elert, A.M., Wörner, M., Braun, U., Klein, R. & Paulus, M. (2017) Assuring quality in microplastic monitoring: About the value of clean-air devices as essentials for verified data. *Scientific Reports*, 7, 5424.
<https://doi.org/10.1038/s41598-017-05838-4>
- Yang, Z. (1994) Maximum likelihood phylogenetic estimation from DNA sequences with variable rates over sites: approximate methods. *Journal of Molecular Evolution*, 39, 306–314.
- Zhang, J., Kapli, P., Pavlidis, P. & Stamatakis, A. (2013) A general species delimitation method with applications to phylogenetic placements. *Bioinformatics*, 29, 2869–2876.
<https://doi.org/10.1093/bioinformatics/btt499>